

# Photoredox autocatalysis: towards a library of generally applicable reductive photocatalysts

Jaspreet Kaur,<sup>1†</sup> Mark John P. Mandigma,<sup>1†</sup> Nakul Bapat,<sup>1</sup> Joshua P. Barham\*<sup>1</sup>

<sup>1</sup>Institute of Organic Chemistry, University of Regensburg, Universitätsstr. 31, 93053 Regensburg (Germany)

\*E-mail: [Joshua-Philip.Barham@chemie.uni-regensburg.de](mailto:Joshua-Philip.Barham@chemie.uni-regensburg.de)

<sup>†</sup>These authors contributed equally.

**Abstract:** Dichotomous thinking dominates the field of synthetic photochemistry – either a reaction needs a photocatalyst or not. Herein, we report the discovery of photoredox autocatalytic pathway, a third mechanistic paradigm that is thus far overlooked, to access cyclic biaryl sulfonamides (**BASNs**). This reaction does not require exogenous catalyst as the visible light absorbing deprotonated product itself, with potent excited state reductive power, acts as the photocatalyst for its own synthesis. This finding implicated **BASN** as a novel organophotocatalyst architecture and allowed a rapid, modular, and low-cost combinatorial synthesis of a **BASN** library that expedited optimal photocatalyst screening. Furthermore, **BASN** was revealed as a general organophotocatalyst for a diverse set of transition metal-free transformations such as: intramolecular (spiro)-cyclizations, defunctionalizations, and C-C / C-heteroatom couplings.

## Introduction

The use of visible light to drive chemical reactions has been one of the most successful contemporary advances in organic synthesis. Notably, it has allowed redox and radical chemistries to flourish and paved ways to rapidly access molecular complexities by open-shell mechanisms that are rather difficult to achieve otherwise<sup>1–5</sup>. Accessing radical intermediates by photo-induced single electron transfer (SET) is dominated by two popular strategies: i) photoredox catalysis, where a catalytic chromophore is used to harvest energy from light to induce SET events<sup>6–8</sup> and ii) photocatalyst-free reactions such as irradiation of visible light absorbing substrates or electron donor and acceptor (EDA) complexes<sup>9–12</sup>, where stoichiometric reagents are involved (Figure 1A, left). Both have their own advantages and drawbacks. For example, the former strategy enjoys the redox activation of non-photo absorbing substrates but requires an initial effort of screening appropriate photocatalysts which are often expensive or can require elaborate synthesis. On the other hand, the latter strategy boasts a green and cost-effective alternative (as it is photocatalyst free) but requires reactants to either be sufficiently photo-absorbing or electronically biased such that they form photo-absorbing complexes. Unbeknownst to many, there is a process that has the intermediary characteristics of the two, whereby no external photocatalyst is needed at the start of the reaction but as the product accumulates, the reaction accelerates<sup>13,14</sup>. As such, it inherits both the assets of the aforementioned popular pathways. This third process is called photoredox autocatalysis, where an intermediate or a product of a reaction acts as the photocatalyst for its own formation (Figure 1A, right). Thermally, autocatalysis is an important process found in biochemical pathways and is often attributed as the primordial method to access chirality<sup>15–19</sup>. Moreover, this was observed in organo-zinc reactions (i.e., Soai reaction)<sup>20–24</sup>, cycloadditions<sup>25,26</sup>, directed *ortho*-lithiation<sup>27</sup>, and supramolecular chemistry<sup>28,29</sup>. However, autocatalysis has thus far enjoyed limited attention and practical applications in the field of synthetic photochemistry<sup>30–33</sup> – therefore the need to fill this knowledge gap is apparent and timely.

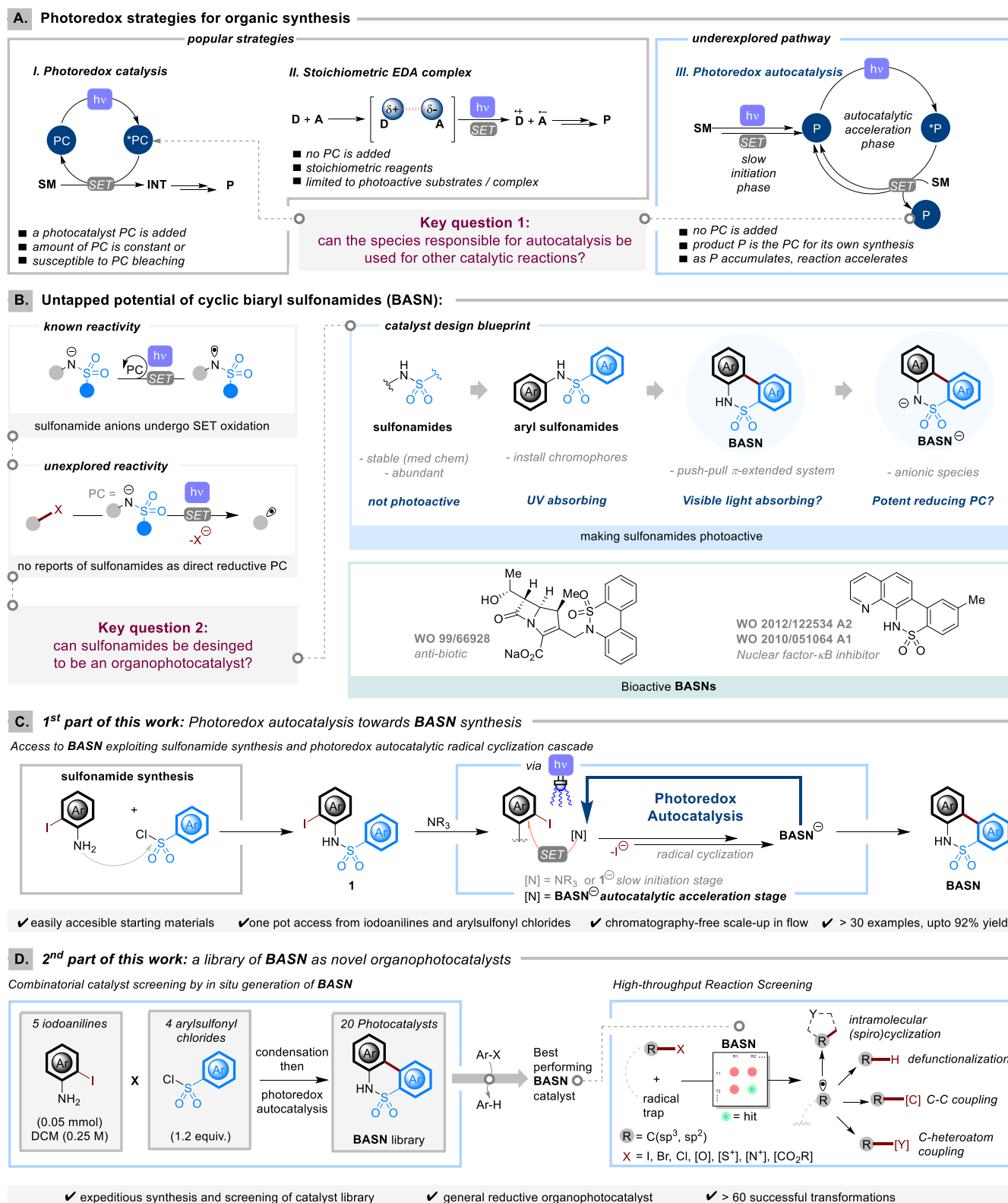


**Figure 1.** Key concepts on autocatalysis and sulfonamide chemistry to be explored in this study.

In recent years, organophotocatalysts have proven to be a viable alternative to traditional precious transition-metal photocatalysts. In line with this, many research groups aspire to design an organophotocatalyst scaffold that is easy to prepare and has desirable photophysical and redox properties<sup>34</sup>. Inspired by the prominence of sulfonamides in medicinal chemistry, due to their rigidity and exceptional chemical/metabolic stability, we reasoned that sulfonamide containing moieties would be good candidates for inexpensive, stable photocatalyst frameworks. Interestingly, the sulfonamidyl functionality in photocatalyst structure is unprecedented as its reactivity mainly involves the applications of *N*-centered radicals (i.e. as hydrogen atom transfer, HAT, agents) which require a preliminary oxidation step (e.g. Hofmann–Löffler type reaction, proton coupled electron transfer, photochemical or electrochemical oxidation)<sup>35–40</sup>. Nevertheless, the ease of sulfonamidyl anion oxidation is an attractive starting point for a catalyst design<sup>41</sup> (Figure 1B, left). Intuitively, incorporation of aryl groups as chromophores at sulfonamide's nitrogen and sulfonyl groups would make the compound photoactive in the UV-B/A region (Figure 1B, top right). Furthermore, we posited that by simply connecting these aryl groups as a cyclic biaryl sulfonamide (henceforth abbreviated as **BASN**) might set up a push-pull extended  $\pi$  electronic system shifting the absorption to the visible region. With this catalyst design at hand and considering that **BASNs** themselves are emerging bioactive compounds (Figure 1B, bottom right), we sought to investigate **BASN**'s synthetic and catalytic potential.

In this study, we discovered the photoredox autocatalytic pathway towards **BASN** – this further supported the use of **BASN** as a photocatalyst together with the abovementioned blueprint (Figure 1C). In other words, as **BASN** can act as a photocatalyst for its own formation, logic follows that it could be employed as a photocatalyst for other reactions. Exploiting the ease of synthesis of **BASN**, a rapid combinatorial design allowed one-pot, *in situ* generation of diverse **BASN** photocatalysts from inexpensive, easily accessible building blocks. This photocatalyst library was then directly screened in photo-reductive transformations and as such this design enabled rapid identification of the optimal photocatalyst structure. Through high-throughput reaction screening, we tested **BASN**'s applicability to catalyze diverse transition metal-free radical transformations (Figure 1D) such as: i) intramolecular (spiro)-cyclizations, ii) defunctionalizations, and iii) C-C / C-heteroatom couplings.

### Reaction development and discovery of photoredox autocatalysis

Considering cost and ease of reaction, we planned to synthesize **BASN** starting with simple condensation of readily-accessible iodoanilines and aryl sulfonyl chlorides, followed by radical cyclization (see section 5.1 of Supporting Information, SI, for retrosynthesis and cost analysis). At the onset of the study, we investigated the reductive radical cyclization of tosylated *o*-iodoaniline **1a** induced by SET reduction of the aryl iodide by a radical anionic organophotocatalyst generated upon visible light irradiation (Figure 2A). Catalytic loadings of 4CzIPN or NpMI gave **BASN** product **2a** in 52% and 50% respectively. However, we were surprised that the reaction worked even without a photocatalyst – affording **2a** in 34%. Even more so, the yield of **2a** improved (to 40%) by irradiation of the reaction mixture containing only **1a** and tributylamine (i.e., in the absence of a photocatalyst and an inorganic base). After design of experiment (DoE) optimization and further screening of conditions (see section 5.2 of SI for full details), we identified that the use of *N,N*-dimethylethanolamine (DMEA) under blue light irradiation ( $h\nu = 450$  nm) afforded **2a** in a high yield (84%) within short reaction time of 3 h. Furthermore, fluorine-containing **BASN 2b**,

was accessed in excellent yield (91%) under these conditions. Control reactions confirmed that both light and DMEA are crucial for this transformation.

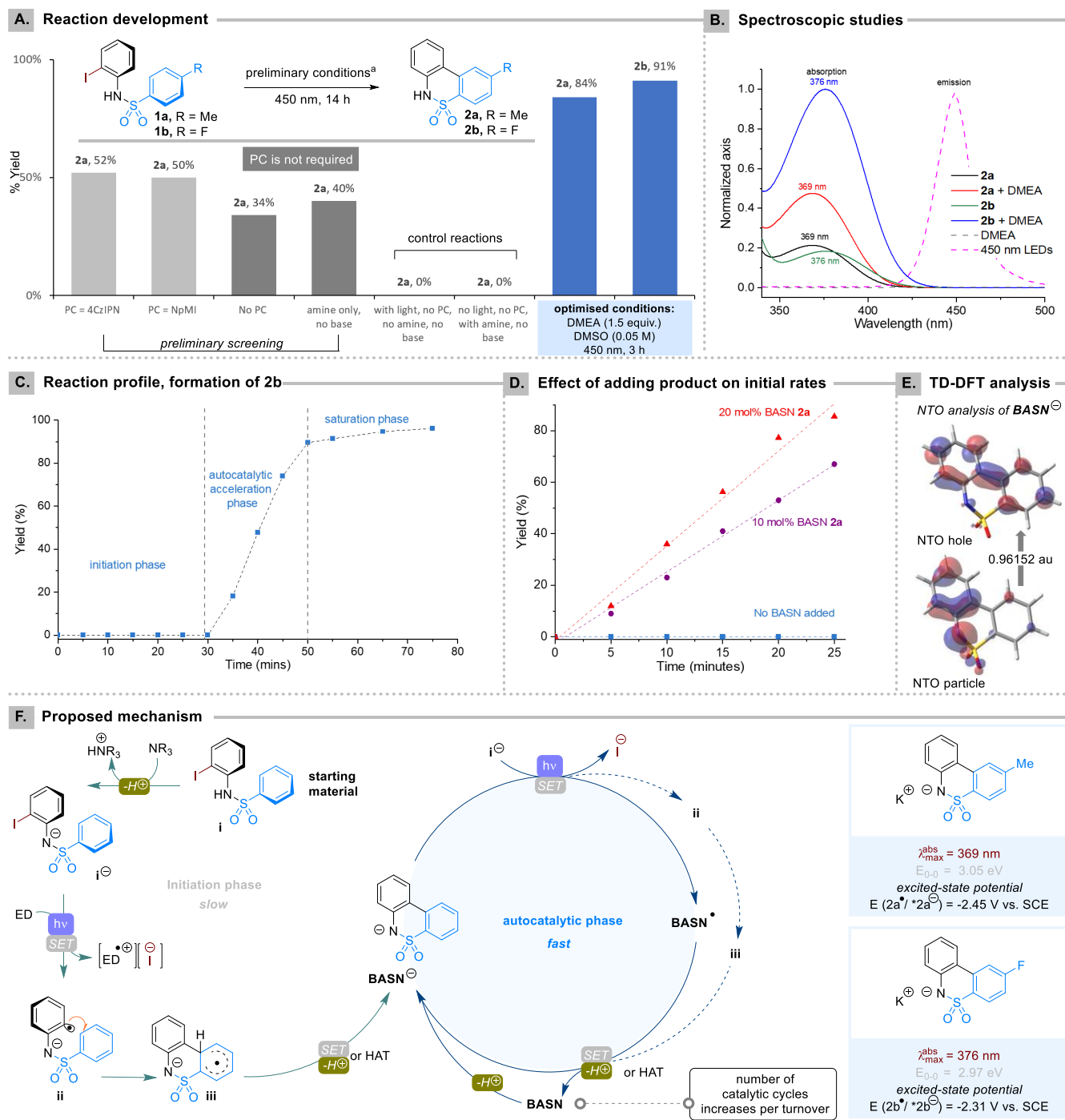


**Figure 2.** <sup>a</sup> K<sub>2</sub>HPO<sub>4</sub> (2 equiv.), amine = NBu<sub>3</sub> (2 equiv.), PC (5 mol%), DMSO:H<sub>2</sub>O (9:1), see SI for optimization details and amine screening. ED = electron donor.

Intrigued by the efficiency of this reaction and the fact that exogenous photocatalyst is not required, the mechanism was then probed (see section 6 of SI for full mechanistic analysis). The reaction profile for the consumption of **1b** / formation of **2b** (monitored using <sup>19</sup>F-NMR) displayed a sigmoidal shape (Figure 2C) and its second derivative fits a parabolic trend (see SI, Figure S15). This establishes that the reaction has three phases: slow initiation, acceleration (with the maximum rate reach when [**1b**] = [**2b**]), and a saturation phase – hallmarks of

an autocatalytic process<sup>13,14,42</sup>. To check this, we performed the unequivocal test for autocatalysis which involves the effect of the adding product on the initial rates<sup>14</sup>. Therefore, **2a** was added<sup>43</sup> at increasing catalytic loadings: 0 mol%, 10 mol%, and 20 mol% (Figure 2D). Indeed, the initial rate for formation of **2b** (i.e., slope of the yield as a function of time) increases as the loading of **BASN 2a**. UV-Vis spectroscopy revealed that the deprotonated product is the most light absorbing species at the blue region tailing until ca. 450 nm, catching the tail end of the emission of the 450 nm LED employed (Figure 2B). <sup>1</sup>H-NMR studies confirmed that the sulfonamide moieties of **1** and **2** are deprotonated under the reaction conditions, consistent with the pKas of arylsulfonamides (pKa of **1a** = 8.1 and pKa of **2a** = 8.9),<sup>44</sup> and DMEA (pKaH = 9.23)<sup>45</sup>. Taken together, we propose that deprotonated **2** is the active photocatalyst in its own autocatalytic synthesis that engages **1** in electron transfer. Consistent with this proposal, testing an *N*-methylated sulfonamide that cannot be deprotonated afforded **3a** (*vide infra*) only in trace amounts. Repeating the same reaction by adding catalytic amount of **2a** considerably increased the yield to 48% (see SI, section 6.8).

Considering the electron rich nature of the aryl iodide of deprotonated **1**, we believe that it undergoes a concerted dissociative SET reduction (meaning there will be no radical dianion intermediate) following the Marcus Savéant theory, directly affording the aryl radical intermediate<sup>46–48</sup>. Density Functional Theory (DFT) calculations revealed that the most favorable SET donor present would be the deprotonated product **BASN<sup>-</sup>** (See section 6.12 of SI). Time Dependent Density Functional Theory (TD-DFT) analysis of **BASN<sup>-</sup>**'s longest wavelength excitation revealed a  $\pi \rightarrow \pi^*$  transition involving charge transfer from the electron rich aniline moiety across the entire electron poor biaryl moiety (Figure 2E); such a charge transfer is reminiscent of a typical organophotocatalyst excitation<sup>49</sup>.

From the UV-Vis, cyclic voltammetry (CV), and emission experiments, it was estimated that **\*BASNs 2a<sup>-</sup>** and **2b<sup>-</sup>** can reach excited state redox potentials of -2.45 V and -2.31 V versus SCE respectively<sup>50</sup> (see section 6.5 of SI). A quantum yield measurement of less than 0.5% suggests a radical chain mechanism is unlikely<sup>51</sup>. From these experiments, we propose the following photoredox autocatalytic cycle (Figure 2F). After deprotonation of the starting material **i**, a mildly photo-absorbing anionic intermediate **i<sup>-</sup>** is excited by light. A concerted dissociative SET from DMEA or another equivalent of **i<sup>-</sup>** generates aryl radical intermediate **ii**, followed by de-aromatic *ortho* cyclization to form **iii**. Rearomatization by SET and deprotonation or by HAT affords a deprotonated **BASN<sup>-</sup>** product, marking the end of a slow initiation phase. Once the **BASN<sup>-</sup>** is present in the system, this acts as an autocatalyst for a redox-neutral cyclization of another equivalent of **i<sup>-</sup>**, intercepting the catalytic cycle again after aryl radical generation and re-aromatization. This autocatalytic phase is faster as i) **BASN<sup>-</sup>** has the most efficient absorption at the blue region, ii) packs the highest reductive redox power in its excited state, and iii) the photocatalyst concentration increases with every turnover.

After the photoredox autocatalytic nature of the reaction was established, the scope of self-synthesizing **BASNs** was examined (Figure 3). We were delighted to find generally high (up to 92%) yields and the library of structures (photocatalysts) is broad (34 examples), with varying the electronics and positions of the substituents on the aryl sulfonyl group (**2a** to **2p**) and aminoaryl group (**2q** to **2ad**). This suggests the photoredox autocatalytic phase is much more generally applicable than anticipated. Exceptions were present such as **2h** and **2o** which were

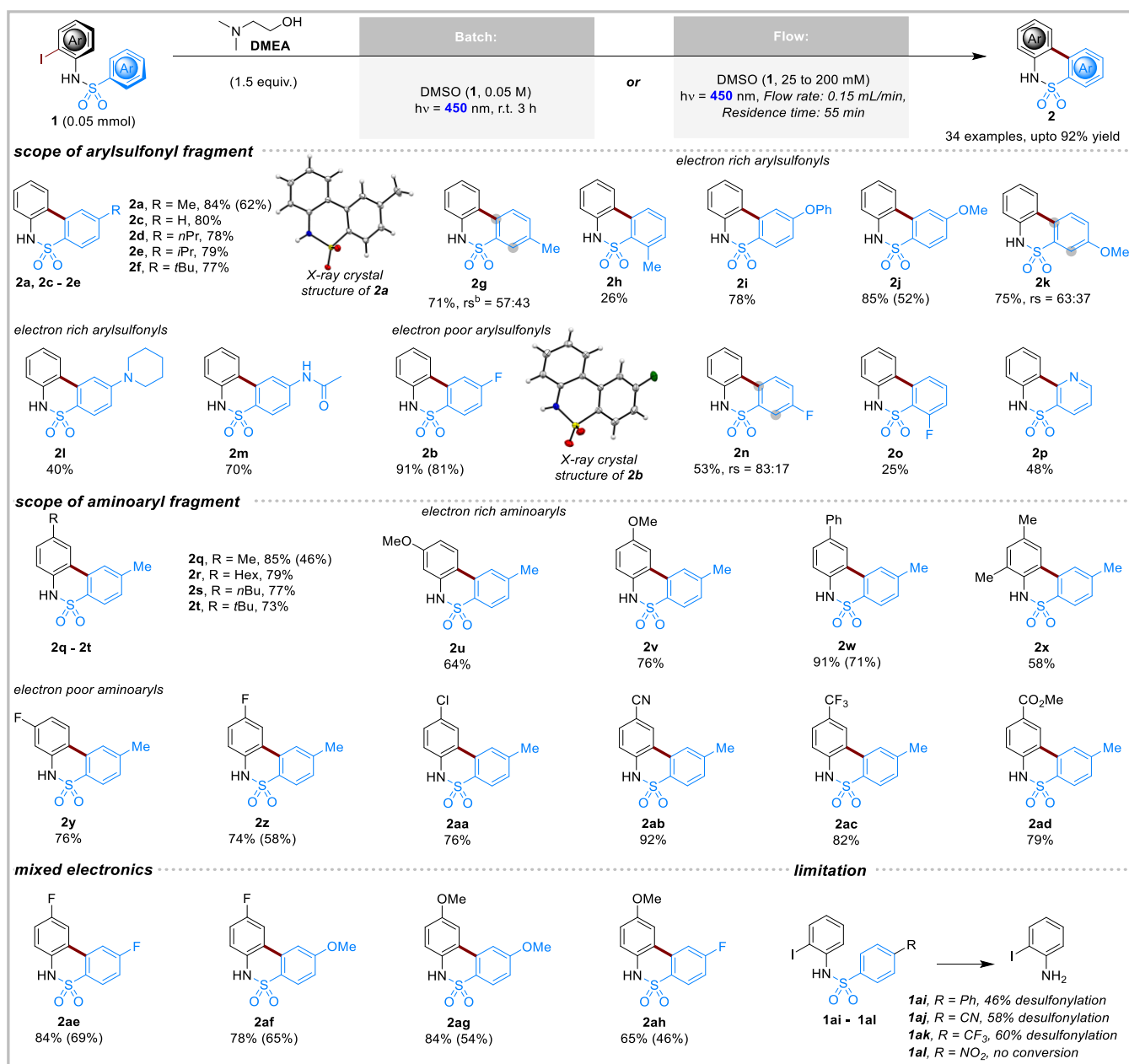


**Figure 3.** Substrate scope of photoredox autocatalytic BASN synthesis. Yields obtained with flow (See section 7 of SI for details of reaction conditions) are inside the parenthesis. *rs* = regioselectivity ratio where the regio-isomer connectivity are indicated by the grey circle with the major isomer as drawn.

afforded in relatively low yields as *ortho*-substituents on the aryl sulfonyl side promoted a Smiles-Truce rearrangement<sup>52,53</sup>. Substrates bearing aryl sulfonyls which are too electron poor or with extended conjugation were not well-tolerated as either desulfonylation (**1ai** to **1ak**) or no reaction (**1al**) was observed. Representative examples (**2a**, **2b**, **2j**, **2q**, **2w**, **2z**, **2ae**, **2af**, **2ag**, and **2ah**) were accessed on a semi-preparative scale using a commercially available photo-flow reactor without optimization in moderate to high yields (Figure 3, yields in parenthesis).

To further challenge the practicality of this method, we examined scalability, use of direct sunlight, and plausibility of a one-pot BASN synthesis (Figure 4). Gram scale (10 mmol) synthesis of **2b** was demonstrated in

flow, affording a high yield (81%) and decent productivity (3 g/day). To our delight, we were also able to harness energy from sunlight on a fair day for a 5 mmol preparative scale synthesis of **2a**, achieving a good yield (65%). Finally, we showcased a telescope synthesis of **2a** directly from commercially-available *o*-iodoaniline **4** and tosyl chloride **5** without much erosion of yield (73%) compared to the single-step process.

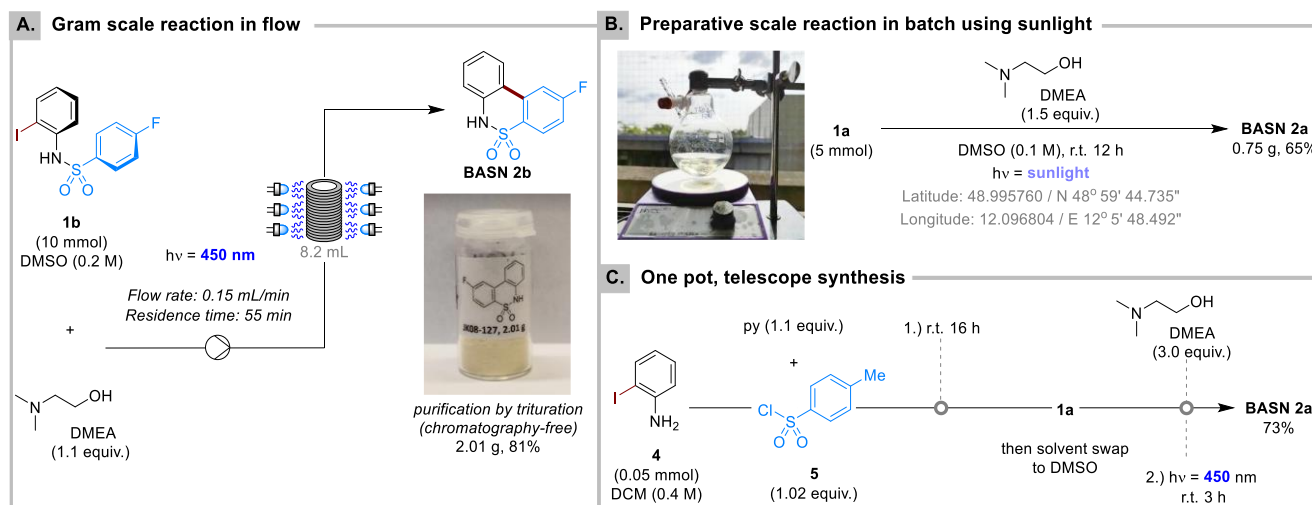


**Figure 4.** A) BASN synthesis: scale-up in flow; B) sunlight irradiation in batch; and C) telescope synthesis. py = pyridine.

Considering **BASN**'s photophysical and reductive properties (*vide supra*), we investigated its use as a photocatalyst. We chose reductive de-functionalization of aryl halides methyl 2-chlorobenzoate (-2.00 V vs SCE)<sup>54</sup> and 4-bromobiphenyl (-2.4 V vs SCE)<sup>55</sup> as our model reactions. Taking advantage of the successful telescope synthesis of **BASN** and to expedite the determination of the best **BASN** structure for reductive de-functionalization, a combinatorial catalyst screening approach was designed whereby nine building blocks (i.e., five sulfonyl chlorides and four iodo-anilines) were used to assemble a library of 20 **BASN** structures in parallel by telescoped sulfonamide synthesis and photoredox autocatalytic cyclization (Figure 5A). Subsequently, the reductive de-functionalization of aryl halides was tested in these *in situ* generated photocatalysts and the results are outlined in Figure 5B. While all 20 catalyst structures performed well with the activated aryl chloride substrate (yield 81 to >99%, see SI, Figure S28), the variation in catalytic performance was more pronounced when model substrate 4-bromobiphenyl was used which has a deeper reduction potential. Here, the best performing photocatalyst is **BASN 2b**. We recognize

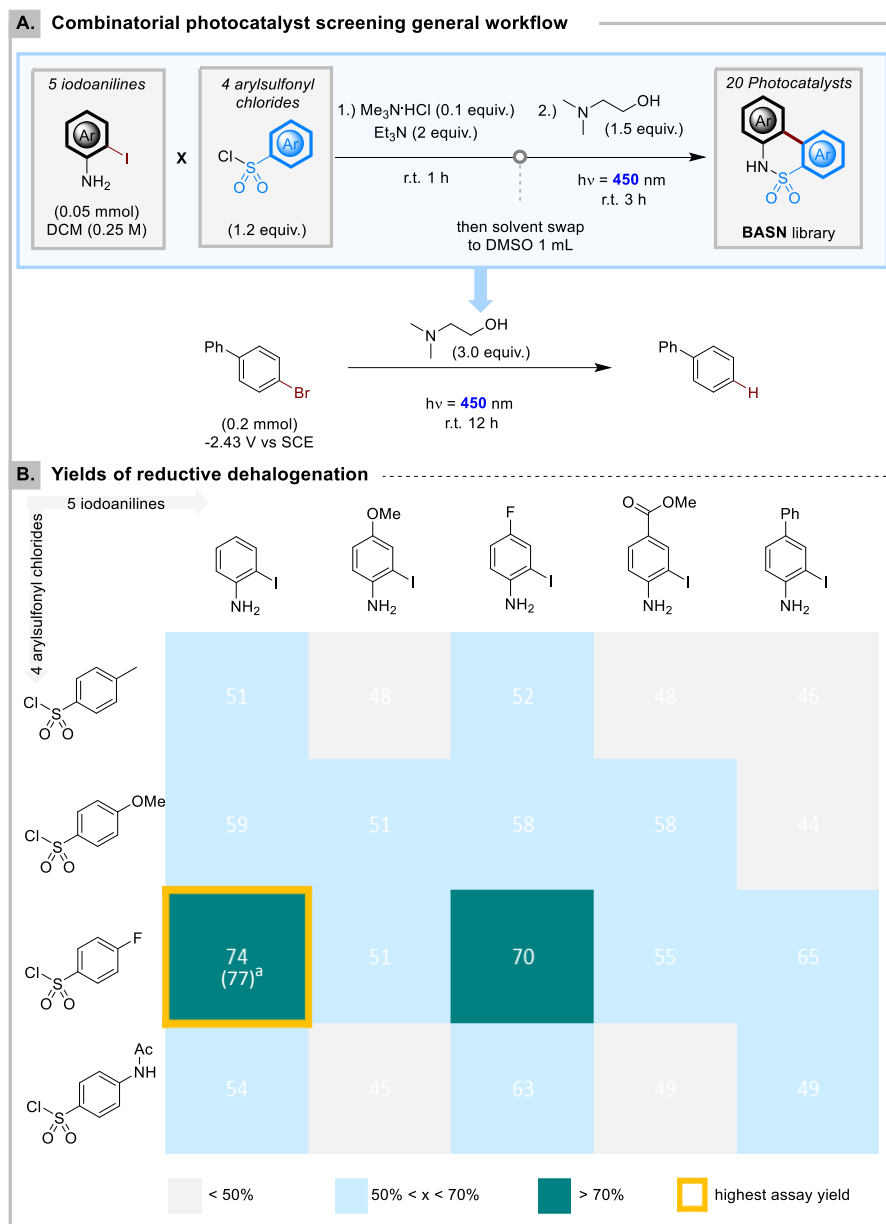


**Figure 5.** Combinatorial catalyst screening. <sup>a</sup>Confirmatory experiment using 10 mol% of **2b**.

that the efficiencies of the photoredox autocatalytic step might differ between catalysts, leading to different final catalyst concentrations. However, the reductive defunctionalization reaction was fairly insensitive to catalyst loading as the yield of debromination does not correlate with the amount of the catalyst present ( $R^2 = 0.0519$ , see SI, Figure S30). Furthermore, a confirmatory experiment affording 77% of the biphenyl product using 10 mol% of **BASN 2b** is at par with the result from the library screening. A control experiment employing *N*-phenyl-*p*-toluenesulfonamide as a catalyst did not yield de-halogenated product, confirming the cyclic biaryl scaffold is important for the photocatalytic performance.

After identifying **BASN 2b** as the best photocatalyst, it was used for the synthesis of several other heterocyclic structures (whose products or intermediates are incapable of autocatalysis), exploiting the generation of aryl-

radicals from aryl iodides followed by intramolecular cyclization (Figure 6). Examples include six-membered methylated biaryl sultams (**3a** and **3b**), and biaryl sultones (**3c** to **3e**). Keeping in mind pharmaceutically-relevant ring systems, we synthesized novel seven-membered cyclic biaryl variants (**3f** to **3i**) and assembled spirocyclic structures via a cascade of aryl radical generation followed by 1,5-HAT and then radical cyclization (**6a** to **6k**).

To further investigate the generality of **BASN** as a reductive organophotocatalyst, a high throughput reaction screening<sup>56,57</sup> was conducted (see section 9 of SI). Good hits for reductive activation were obtained for a selection of radical precursors among which include aryl halides, benzoic esters, *N*-(acyloxy)phthalimides, Katritzky

salt, Togni's reagent II (**Tr-II**), and aryl sulfonium salt (Figure 7A). Figure 7B outlines examples for reductive defunctionalizations such as dehalogenations of aryl chlorides, bromides, and iodides (**7a to 7c**), detosylations (**7e** and **7f**), and deoxygenations of trifluoromethylated benzoate esters (**7g** and **7h**). Next, we turned our attention to complexity-building reactions such as transition metal-free C-C couplings of alkyl, aryl and trifluoromethyl radical precursors with olefins or heterocycles (Figure 7C) affording Heck-type products (**8a to 8o**). Interestingly, removing the base gave better yields with *N*-(acyloxy)phthalimides (**8a to 8i**) which could be attributed to a favorable catalyst-substrate preassembly via synergistic H-bond and  $\pi$ -stacking that assisted a photoinduced intra-complex electron transfer (Figure 7C.1, Figure S32 for the yields with base, and section 6.12 of SI for computational investigations on these non-covalent interactions). Activation and C-heteroatom coupling of aryl chlorides was also demonstrated (Figure 7D) obtaining phosphorylation (**9a to 9k**), borylation (**9l** and **9m**), and sulfidation (**9n** and **9o**) products. Late-stage diversification of industrially-relevant molecules (gemfibrozil **8h** and **8j**, caffeine **8o**, boscalid **9k**, and menthol **9m**) and introduction of benzene bio-isosteres bicyclo[1.1.1]pentane (BCP) **8g** and bicyclo[2.2.2]octane (BCO) **8f** and **8i** were demonstrated, further highlighting the synthetic utility of this method.

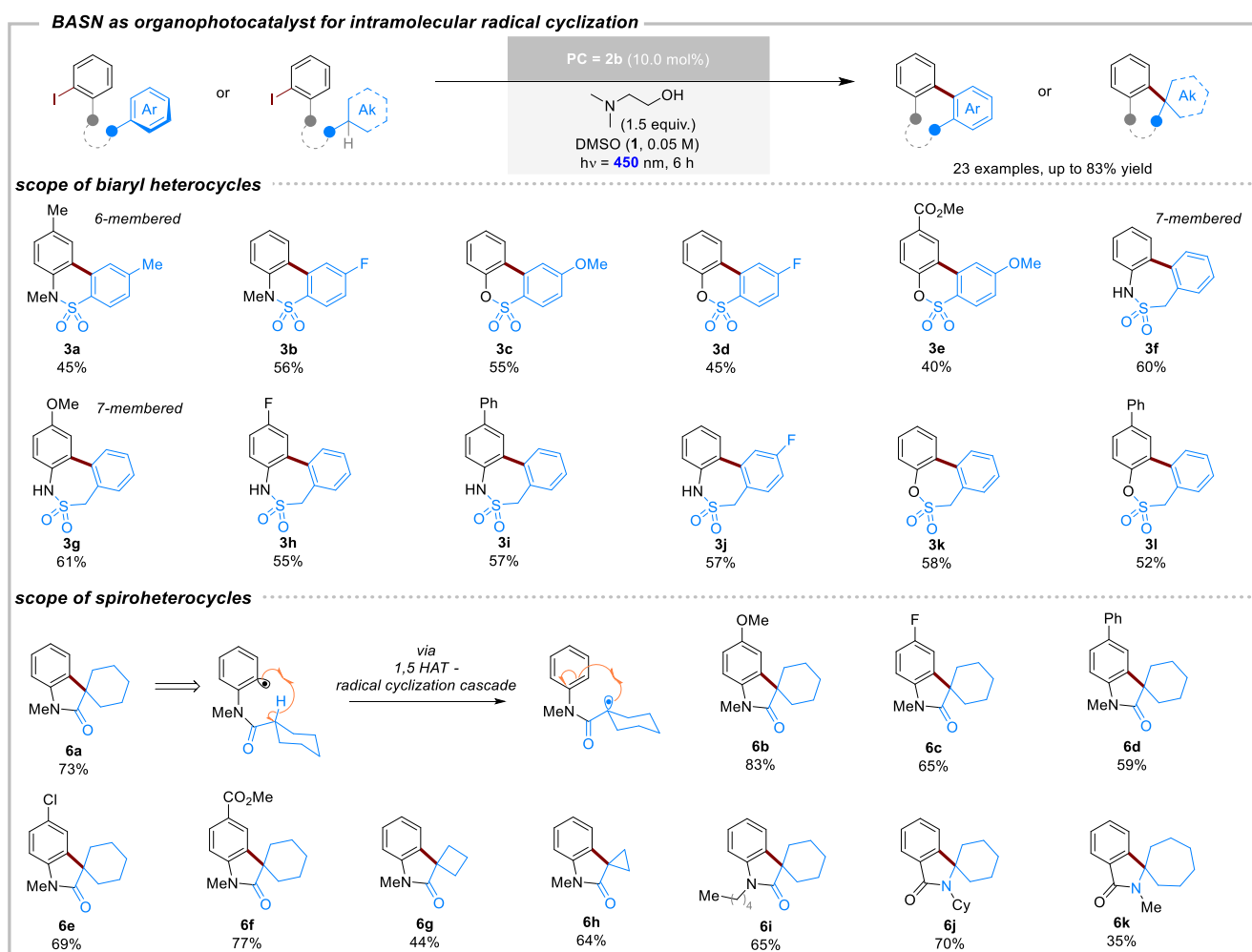


**Figure 6.** Synthesis of heterocycles via visible light promoted radical cyclization using **BASN** as organophotocatalyst.

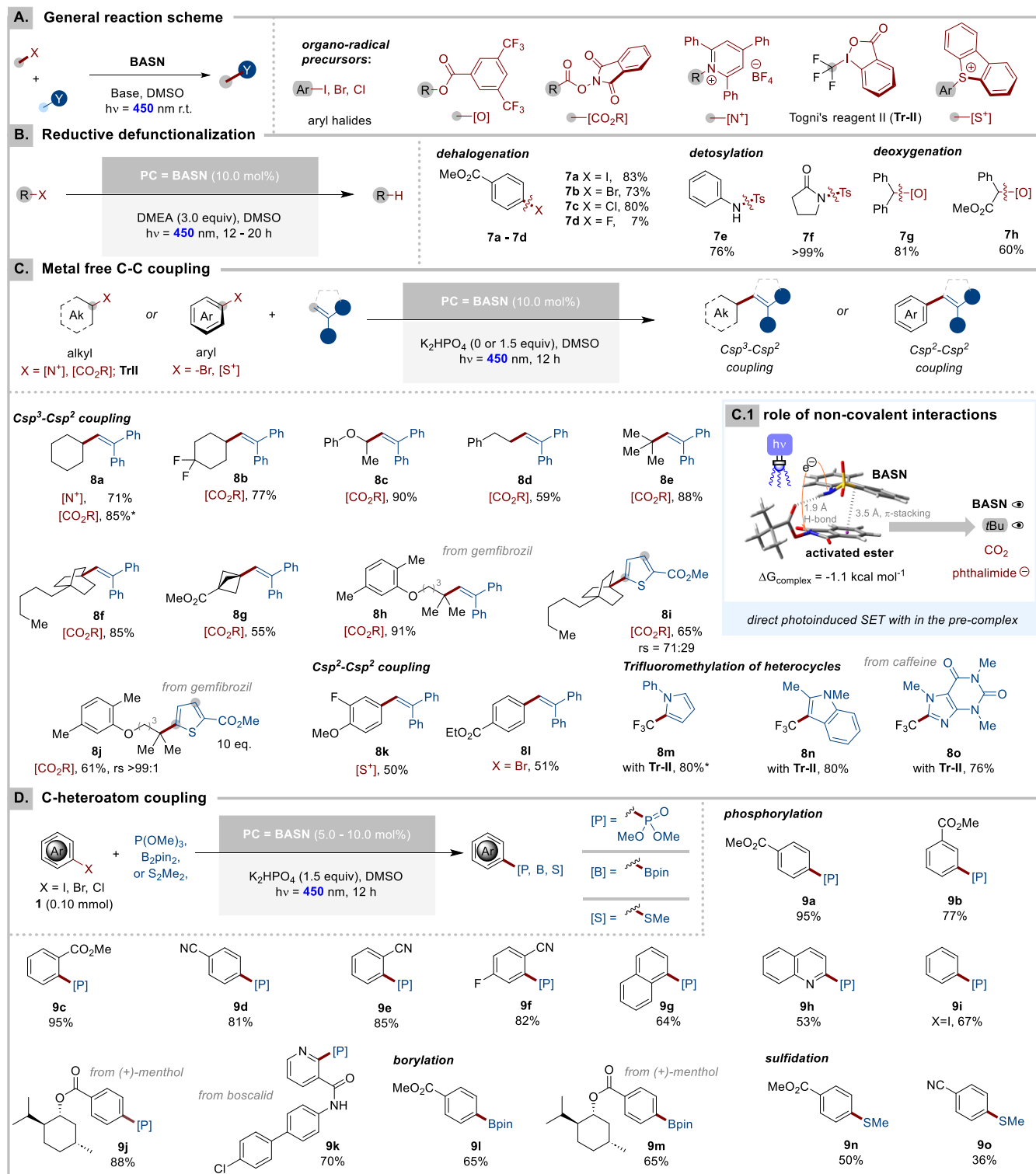


**Figure 7.** BASN as a general reductive organophotocatalyst. rs = regioselectivity ratio where the regio-isomer connectivity are indicated by the grey circle with the major isomer as drawn.

In conclusion, this study outlines the underexplored third mechanistic paradigm in electron transfer photochemistry – photoredox autocatalysis. In turn, this allowed the development of **BASN** as a novel and generally

applicable reductive organophotocatalyst architecture that is easily diversifiable and efficiently accessible in a low cost, one-pot process from anilines and sulfonyl chlorides. Due to the ubiquity of the precursors and the privileged role of sulfonamides and biaryls as robust, biocompatible motifs in medicinal chemistry, we believe this class of photocatalyst will be of great significance to chemists from industry and academia alike and may pave the way to further biological applications of **BASNs**. We hope that the systematic approach of this study will serve as a blueprint for further development of the budding field of photoredox autocatalysis.

**Acknowledgements** J. K., M. J. P. M. and J. P. B. thank the Alexander von Humboldt Foundation for funding, provided within the framework of the Sofja Kovalevskaja Award endowed to J. P. B. by the German Federal Ministry of Education and Research. J. K. is co-financed by a BDF (Bayerischen Gleichstellungsförderung) Scholarship for which she thanks the Bayerische Staatsministerium für Wissenschaft und Kunst. N. B. thanks the German Academic Exchange Service (DAAD) for a DAAD-WISE scholarship for N. B.'s research exchange to Universität Regensburg. We thank Regina Hoheisel for assistance and training in cyclic voltammetry, Wolfgang Haumer and Julia Zach for assistance and training in luminescence spectroscopy measurements, Julia Zach for assistance and training in quantum yield measurements, and Birgit Hischa for running X-ray diffraction analyses. J. K. and J. P. B. are members of DFG TRR 325 'Assembly Controlled Chemical Photocatalysis' (444632635) and thank other members of the TRR for insightful discussions.

## References

- (1) Bonfield, H. E.; Knauber, T.; Lévesque, F.; Moschetta, E. G.; Susanne, F.; Edwards, L. J. Photons as a 21st Century Reagent. *Nat Commun* **2020**, *11* (1), 804. DOI: 10.1038/s41467-019-13988-4.
- (2) Ciamician, G. The Photochemistry of the Future. *Science* **1912**, *36* (926), 385–394. DOI: 10.1126/science.36.926.385.
- (3) Prier, C. K.; Rankic, D. A.; MacMillan, D. W. C. Visible Light Photoredox Catalysis with Transition Metal Complexes: Applications in Organic Synthesis. *Chem. Rev.* **2013**, *113* (7), 5322–5363. DOI: 10.1021/cr300503r.
- (4) Schultz, D. M.; Yoon, T. P. Solar Synthesis: Prospects in Visible Light Photocatalysis. *Science* **2014**, *343* (6174), 1239176. DOI: 10.1126/science.1239176.
- (5) Stephenson, C.; Yoon, T. Enabling Chemical Synthesis with Visible Light. *Acc. Chem. Res.* **2016**, *49* (10), 2059–2060. DOI: 10.1021/acs.accounts.6b00502.
- (6) Shaw, M. H.; Twilton, J.; MacMillan, D. W. C. Photoredox Catalysis in Organic Chemistry. *J. Org. Chem.* **2016**, *81* (16), 6898–6926. DOI: 10.1021/acs.joc.6b01449.
- (7) Stephenson, C. R. J.; Yoon, T. P.; MacMillan, D. W. C., Eds. *Visible Light Photocatalysis in Organic Chemistry*; Wiley-VCH Verlag GmbH & Co, 2018. DOI: 10.1002/9783527674145.
- (8) Twilton, J.; Le, C.; Zhang, P.; Shaw, M. H.; Evans, R. W.; MacMillan, D. W. C. The Merger of Transition Metal and Photocatalysis. *Nat. Rev. Chem.* **2017**, *1* (7), 1–19. DOI: 10.1038/s41570-017-0052.
- (9) Crisenza, G. E. M.; Mazzarella, D.; Melchiorre, P. Synthetic Methods Driven by the Photoactivity of Electron Donor-Acceptor Complexes. *J. Am. Chem. Soc.* **2020**, *142* (12), 5461–5476. DOI: 10.1021/jacs.0c01416.

- (10) Kaur, J.; Shahin, A.; Barham, J. P. Photocatalyst-Free, Visible-Light-Mediated C(sp<sup>3</sup>)-H Arylation of Amides via a Solvent-Caged EDA Complex. *Org. Lett.* **2021**, *23* (6), 2002–2006. DOI: 10.1021/acs.orglett.1c00132.
- (11) Foster, R. Electron Donor-Acceptor Complexes. *J. Phys. Chem.* **1980**, *84* (17), 2135–2141. DOI: 10.1021/j100454a006.
- (12) Rosokha, S. V.; Kochi, J. K. Fresh look at electron-transfer mechanisms via the donor/acceptor bindings in the critical encounter complex. *Acc. Chem. Res.* **2008**, *41* (5), 641–653. DOI: 10.1021/ar700256a.
- (13) Bissette, A. J.; Fletcher, S. P. Mechanisms of Autocatalysis. *Angew. Chem. Int. Ed.* **2013**, *52* (49), 12800–12826. DOI: 10.1002/anie.201303822.
- (14) Horváth, A. K. Correct Classification and Identification of Autocatalysis. *Phys. Chem. Chem. Phys.* **2021**, *23* (12), 7178–7189. DOI: 10.1039/d1cp00224d.
- (15) Blackmond, D. G. An Examination of the Role of Autocatalytic Cycles in the Chemistry of Proposed Primordial Reactions. *Angew. Chem. Int. Ed.* **2009**, *48* (2), 386–390. DOI: 10.1002/anie.200804565.
- (16) Harmsel, M. ter; Maguire, O. R.; Runikhina, S. A.; Wong, A. S. Y.; Huck, W. T. S.; Harutyunyan, S. R. A Catalytically Active Oscillator Made from Small Organic Molecules. *Nature* **2023**, *621* (7977), 87–93. DOI: 10.1038/s41586-023-06310-2.
- (17) Howlett, M. G.; Fletcher, S. P. From Autocatalysis to Survival of the Fittest in Self-Reproducing Lipid Systems. *Nat. Rev. Chem.* **2023**, *7* (10), 673–691. DOI: 10.1038/s41570-023-00524-8.
- (18) Avalos, M.; Babiano, R.; Cintas, P.; Jiménez, J. L.; Palacios, J. C. Chiral Autocatalysis: where Stereochemistry Meets the Origin of Life. *Chem. Commun.* **2000** (11), 887–892. DOI: 10.1039/A908300F.
- (19) Lincoln, T. A.; Joyce, G. F. Self-Sustained Replication of an RNA Enzyme. *Science* **2009**, *323* (5918), 1229–1232. DOI: 10.1126/science.1167856.
- (20) Athavale, S. V.; Simon, A.; Houk, K. N.; Denmark, S. E. Demystifying the Asymmetry-Amplifying, Autocatalytic Behaviour of the Soai Reaction Through Structural, Mechanistic and Computational Studies. *Nat. Chem.* **2020**, *12* (4), 412–423. DOI: 10.1038/s41557-020-0421-8.
- (21) Soai, K.; Kawasaki, T.; Matsumoto, A. *Chapter 1. Asymmetric Autocatalysis: The Soai Reaction, an Overview*, 2022. DOI: 10.1039/9781839166273-00001.
- (22) Soai, K.; Shibata, T.; Morioka, H.; Choji, K. Asymmetric Autocatalysis and Amplification of Enantiomeric Excess of a Chiral Molecule. *Nature* **1995**, *378* (6559), 767–768. DOI: 10.1038/378767a0.
- (23) Blackmond, D. G.; McMillan, C. R.; Ramdeehul, S.; Schorm, A.; Brown, J. M. Origins of Asymmetric Amplification in Autocatalytic Alkylzinc Additions. *J. Am. Chem. Soc.* **2001**, *123* (41), 10103–10104. DOI: 10.1021/ja0165133.
- (24) Chinkov, N.; Warm, A.; Carreira, E. M. Asymmetric Autocatalysis Enables an Improved Synthesis of Efavirenz. *Angew. Chem. Int. Ed.* **2011**, *50* (13), 2957–2961. DOI: 10.1002/anie.201006689.
- (25) Semenov, S. N.; Belding, L.; Cafferty, B. J.; Mousavi, M. P. S.; Finogenova, A. M.; Cruz, R. S.; Skorb, E. V.; Whitesides, G. M. Autocatalytic Cycles in a Copper-Catalyzed Azide-Alkyne Cycloaddition Reaction. *J. Am. Chem. Soc.* **2018**, *140* (32), 10221–10232. DOI: 10.1021/jacs.8b05048.
- (26) Wang, B.; Sutherland, I. O. Self-Replication in a Diels–Alder Reaction. *Chem. Commun.* **1997** (16), 1495–1496. DOI: 10.1039/A701573I.
- (27) Singh, K. J.; Hoepker, A. C.; Collum, D. B. Autocatalysis in Lithium Diisopropylamide-Mediated Ortholithiations. *J. Am. Chem. Soc.* **2008**, *130* (52), 18008–18017. DOI: 10.1021/ja807331k.
- (28) Malakoutikhah, M.; Peyralans, J. J.-P.; Colomb-Delsuc, M.; Fanlo-Virgós, H.; Stuart, M. C. A.; Otto, S. Uncovering the Selection Criteria for the Emergence of Multi-Building-Block Replicators from Dynamic Combinatorial Libraries. *J. Am. Chem. Soc.* **2013**, *135* (49), 18406–18417. DOI: 10.1021/ja4067805.

- (29) Cullen, W.; Metherell, A. J.; Wragg, A. B.; Taylor, C. G. P.; Williams, N. H.; Ward, M. D. Catalysis in a Cationic Coordination Cage Using a Cavity-Bound Guest and Surface-Bound Anions: Inhibition, Activation, and Autocatalysis. *J. Am. Chem. Soc.* **2018**, *140* (8), 2821–2828. DOI: 10.1021/jacs.7b11334.
- (30) Kim, S.; Martínez Dibildox, A.; Aguirre-Soto, A.; Sikes, H. D. Exponential Amplification Using Photoredox Autocatalysis. *J. Am. Chem. Soc.* **2021**, *143* (30), 11544–11553. DOI: 10.1021/jacs.1c04236.
- (31) Kim, S.; Sikes, H. D. Dual Photoredox Catalysis Strategy for Enhanced Photopolymerization-Based Colorimetric Biodetection. *ACS Appl. Mater. Interfaces* **2021**, *13* (48), 57962–57970. DOI: 10.1021/acsami.1c17589.
- (32) Wang, C.; Zhang, H.; Wells, L. A.; Liu, T.; Meng, T.; Liu, Q.; Walsh, P. J.; Kozłowski, M. C.; Jia, T. Autocatalytic Photoredox Chan-Lam Coupling of free Diaryl Sulfoximines with Arylboronic Acids. *Nat Commun* **2021**, *12* (1), 932. DOI: 10.1038/s41467-021-21156-w.
- (33) Lancel, M.; Zimmerlin, P.; Gomez, C.; Port, M.; Khrouz, L.; Monnereau, C.; Amara, Z. Self-Sensitized Photooxidation of Naphthols to Naphthoquinones and the Use of Naphthoquinones as Visible Light Photocatalysts in Batch and Continuous Flow Reactors. *J. Org. Chem.* **2023**, *88* (10), 6498–6508. DOI: 10.1021/acs.joc.2c03014.
- (34) Romero, N. A.; Nicewicz, D. A. Organic Photoredox Catalysis. *Chem. Rev.* **2016**, *116* (17), 10075–10166. DOI: 10.1021/acs.chemrev.6b00057.
- (35) Kwon, K.; Simons, R. T.; Nandakumar, M.; Roizen, J. L. Strategies to Generate Nitrogen-centered Radicals That May Rely on Photoredox Catalysis: Development in Reaction Methodology and Applications in Organic Synthesis. *Chem. Rev.* **2022**, *122* (2), 2353–2428. DOI: 10.1021/acs.chemrev.1c00444.
- (36) Ram Bajya, K.; Kumar, M.; Ansari, A.; Selvakumar, S. Sulfonamide as Photoinduced Hydrogen Atom Transfer Catalyst for Organophotoredox Hydrosilylation and Hydrogermylation of Activated Alkenes. *Adv Synth Catal* **2023**, *365* (7), 976–982. DOI: 10.1002/adsc.202300040.
- (37) Tang, N.; Wu, X.; Zhu, C. Practical, Metal-Free Remote Heteroarylation of Amides via Unactivated C(sp<sup>3</sup>)-H Bond Functionalization. *Chem. Sci.* **2019**, *10* (28), 6915–6919. DOI: 10.1039/c9sc02564b.
- (38) Pratley, C.; Fenner, S.; Murphy, J. A. Nitrogen-Centered Radicals in Functionalization of sp<sup>2</sup> Systems: Generation, Reactivity, and Applications in Synthesis. *Chem. Rev.* **2022**, *122* (9), 8181–8260. DOI: 10.1021/acs.chemrev.1c00831.
- (39) Tanaka, H.; Sakai, K.; Kawamura, A.; Oisaki, K.; Kanai, M. Sulfonamides as New Hydrogen Atom Transfer (HAT) Catalysts for Photoredox Allylic and Benzylic C-H Arylations. *Chem. Commun.* **2018**, *54* (26), 3215–3218. DOI: 10.1039/c7cc09457d.
- (40) Teng, X.; Yu, T.; Shi, J.; Huang, H.; Wang, R.; Peng, W.; Sun, K.; Yang, S.; Wang, X. Recent Advances in the Functionalization of Remote C–H Bonds by Hofmann-Löffler-Freytag-type Reactions. *Adv. Synth. Catal.* **2023**, *365* (19), 3211–3226. DOI: 10.1002/adsc.202300718.
- (41) Schmalzbauer, M.; Marcon, M.; König, B. Excited State Anions in Organic Transformations. *Angew. Chem. Int. Ed.* **2021**, *60* (12), 6270–6292. DOI: 10.1002/anie.202009288.
- (42) Hanopolskyi, A. I.; Smaliak, V. A.; Novichkov, A. I.; Semenov, S. N. Autocatalysis: Kinetics, Mechanisms and Design. *ChemSystemsChem* **2021**, *3* (1), e2000026. DOI: 10.1002/syst.202000026.
- (43) here, a non-fluorinated species was chosen as to not interfere with <sup>19</sup>F-NMR signal giving the true yield of 2b.
- (44) Pan, X.; Wang, H.; Li, C.; Zhang, J. Z. H.; Ji, C. MolGpka: A Web Server for Small Molecule pKa Prediction Using a Graph-Convolutional Neural Network. *J. Chem. Inf. Model.* **2021**, *61* (7), 3159–3165. DOI: 10.1021/acs.jcim.1c00075.

- (45) Littel, R. J.; Bos, M.; Knoop, G. J. Dissociation Constants of Some Alkanolamines at 293, 303, 318, and 333 K. *J. Chem. Eng. Data* **1990**, *35* (3), 276–277. DOI: 10.1021/je00061a014.
- (46) Costentin, C.; Robert, M.; Savéant, J.-M. Electron transfer and bond breaking: Recent advances. *Chem. Phys.* **2006**, *324* (1), 40–56. DOI: 10.1016/j.chemphys.2005.09.029.
- (47) Pause, L.; Robert, M.; Savéant, J.-M. Can Single-Electron Transfer Break an Aromatic Carbon–Heteroatom Bond in One Step? A Novel Example of Transition between Stepwise and Concerted Mechanisms in the Reduction of Aromatic Iodides. *J. Am. Chem. Soc.* **1999**, *121* (30), 7158–7159. DOI: 10.1021/ja991365q.
- (48) Saveant, J. M. A Simple Model for the Kinetics of Dissociative Electron Transfer in Polar Solvents. Application to the Homogeneous and Heterogeneous Reduction of Alkyl Halides. *J. Am. Chem. Soc.* **1987**, *109* (22), 6788–6795. DOI: 10.1021/ja00256a037.
- (49) Mandigma, M. J. P.; Kaur, J.; Barham, J. P. Organophotocatalytic Mechanisms: Simplicity or Naïvety? Diverting Reactive Pathways by Modifications of Catalyst Structure, Redox States and Substrate Preassemblies. *ChemCatChem* **2023**, *15* (11). DOI: 10.1002/cctc.202201542.
- (50) Wu, S.; Schiel, F.; Melchiorre, P. A General Light-Driven Organocatalytic Platform for the Activation of Inert Substrates. *Angew. Chem. Int. Ed.* **2023**, *62* (32), e202306364. DOI: 10.1002/anie.202306364.
- (51) Cismesia, M. A.; Yoon, T. P. Characterizing Chain Processes in Visible Light Photoredox Catalysis. *Chem. Sci.* **2015**, *6* (10), 5426–5434. DOI: 10.1039/C5SC02185E.
- (52) Sephton, T.; Large, J. M.; Natrajan, L.; Butterworth, S.; Greaney, M. F. XAT-Catalysis for Intramolecular Biaryl Synthesis. *Angew. Chem. Int. Ed.* **2024**, e202407979. DOI: 10.1002/anie.202407979.
- (53) Hervieu, C.; Kirillova, M. S.; Suárez, T.; Müller, M.; Merino, E.; Nevado, C. Asymmetric, Visible Light-Mediated Radical Sulfinyl-Smiles Rearrangement to Access All-Carbon Quaternary Stereocentres. *Nat. Chem.* **2021**, *13* (4), 327–334. DOI: 10.1038/s41557-021-00668-4.
- (54) Kim, H.; Kim, H.; Lambert, T. H.; Lin, S. Reductive Electrophotocatalysis: Merging Electricity and Light To Achieve Extreme Reduction Potentials. *J. Am. Chem. Soc.* **2020**, *142* (5), 2087–2092. DOI: 10.1021/jacs.9b10678.
- (55) Cowper, N. G. W.; Chernowsky, C. P.; Williams, O. P.; Wickens, Z. K. Potent Reductants via Electron-Primed Photoredox Catalysis: Unlocking Aryl Chlorides for Radical Coupling. *J. Am. Chem. Soc.* **2020**, *142* (5), 2093–2099. DOI: 10.1021/jacs.9b12328.
- (56) McNally, A.; Prier, C. K.; MacMillan, D. W. C. Discovery of an  $\alpha$ -amino C-H Arylation Reaction Using the Strategy of Accelerated Serendipity. *Science* **2011**, *334* (6059), 1114–1117. DOI: 10.1126/science.1213920.
- (57) Strieth-Kalthoff, F.; Henkel, C.; Teders, M.; Kahnt, A.; Knolle, W.; Gómez-Suárez, A.; Dirian, K.; Alex, W.; Bergander, K.; Daniliuc, C. G.; Abel, B.; Guldi, D. M.; Glorius, F. Discovery of Unforeseen Energy-Transfer-Based Transformations Using a Combined Screening Approach. *Chem* **2019**, *5* (8), 2183–2194. DOI: 10.1016/j.chempr.2019.06.004.